

RESEARCH

Open Access



Identification of novel genetic loci related to dromedary camel (*Camelus dromedarius*) morphometrics, biomechanics, and behavior by genome-wide association studies

Carlos Iglesias Pastrana^{1*}, Francisco Javier Navas González¹, Martina Macri^{1,2},
María del Amparo Martínez Martínez¹, Elena Ciani³ and Juan Vicente Delgado Bermejo¹

Abstract

In the realm of animal breeding for sustainability, domestic camels have traditionally been valued for their milk and meat production. However, key aspects such as zoometrics, biomechanics, and behavior have often been overlooked in terms of their genetic foundations. Recognizing this gap, the present study performed genome-wide association analyses to identify genetic markers associated with zoometrics-, biomechanics-, and behavior-related traits in dromedary camels (*Camelus dromedarius*). 16 and 108 genetic markers were significantly associated ($q < 0.05$) at genome and chromosome-wide levels of significance, respectively, with zoometrics- (width, length, and perimeter/girth), biomechanics- (acceleration, displacement, spatial position, and velocity), and behavior-related traits (general cognition, intelligence, and Intelligence Quotient (IQ)) in dromedaries. In most association loci, the nearest protein-coding genes are linked to neurodevelopmental and sensory disorders. This suggests that genetic variations related to neural development and sensory perception play crucial roles in shaping a dromedary camel's physical characteristics and behavior. In summary, this research advances our understanding of the genomic basis of essential traits in dromedary camels. Identifying specific genetic markers associated with zoometrics, biomechanics, and behavior provides valuable insights into camel domestication. Moreover, the links between these traits and genes related to neurodevelopmental and sensory disorders highlight the broader implications of domestication and modern selection on the health and welfare of dromedary camels. This knowledge could guide future breeding strategies, fostering a more holistic approach to camel husbandry and ensuring the sustainability of these animals in diverse agricultural contexts.

Keywords Dromedary camel, Functional traits, Genomic selection

Background

Recognized for their sustainability, domestic camels (dromedaries or one-humped camels (*Camelus dromedarius*) and Bactrian or two-humped camels (*Camelus bactrianus*)) are increasingly raised for various productive purposes worldwide. With a notable demand for camel milk and meat, efforts and strategies focus on growth and milk yield traits. This often sidelines traits like zoometrics, biomechanics, and behavior in genetic

*Correspondence:

Carlos Iglesias Pastrana
ciglesiaspastrana@gmail.com

¹ Department of Genetics, Faculty of Veterinary Sciences, University of Córdoba, Córdoba, Spain

² Animal Breeding Consulting S.L, Parque Científico Tecnológico de Córdoba, Córdoba, Spain

³ Department of Biosciences, Biotechnologies and Environment, Faculty of Veterinary Sciences, University of Bari 'Aldo Moro', Bari, Italy



© The Author(s) 2024. **Open Access** This article is licensed under a Creative Commons Attribution-NonCommercial-NoDerivatives 4.0 International License, which permits any non-commercial use, sharing, distribution and reproduction in any medium or format, as long as you give appropriate credit to the original author(s) and the source, provide a link to the Creative Commons licence, and indicate if you modified the licensed material. You do not have permission under this licence to share adapted material derived from this article or parts of it. The images or other third party material in this article are included in the article's Creative Commons licence, unless indicated otherwise in a credit line to the material. If material is not included in the article's Creative Commons licence and your intended use is not permitted by statutory regulation or exceeds the permitted use, you will need to obtain permission directly from the copyright holder. To view a copy of this licence, visit <http://creativecommons.org/licenses/by-nc-nd/4.0/>.

improvement programs for these animals [1, 2]. Therefore, standardizing the incorporation of these traits into breeding criteria—linked to physical and behavioral performance—will enhance the potential of camels. This is especially relevant for camel breeds and populations used in beauty contests, athletic pursuits (racing and riding), and close interaction with humans (assisted interventions and routine husbandry practices) [3, 4].

In conservation and/or breeding programs, two essential data registries are crucial: phenotypic records of the traits of interest and genealogical information [5]. Estimating individual breeding values using phenotypic and pedigree information is limited for camels due to the lack of traditional pedigrees [6, 7]. To overcome this technical constraint and enhance genetic advancement, efforts are being made to reduce generation intervals [8], which can be achieved by implementing genomics-based selection programs.

Progress in genomic research has provided powerful tools for examining the genetic composition of complex traits and developing selection panels based on genetic markers. This includes single-gene tests [9] and more complex arrays of genetic markers spanning the entire genome, which are known to correlate with specific traits [10]. Genetic polymorphisms of single candidate genes have been proposed in dromedary camels for economically relevant traits such as coat colour [11], udder and body measurements [12–14], and reproductive performance [15].

Complex genetic breeding programs can also be developed using genome-wide association studies (GWAS). For instance, Bitaraf Sani, Zare Harofte [6] identified 99 genome-wide significant SNPs associated with birth weight, daily gain, and body weight in Iranian dromedaries. Within the same animal population, 9 significant SNPs located in 16 candidate genes and 13 significant SNPs located in 24 candidate genes were associated with white and black coat color, respectively [16]. Additionally, Karimi, Burger [17] found 59 SNPs significantly associated with 12 morphometric traits and classified 37 candidate genes in Iranian dromedaries. Moreover, 111 SNPs were identified as significantly associated with weight-for-age traits in Pakistani dromedary camels [18].

However, the genetic basis of other functional traits of economic relevance, such as athletic performance and behavioural features, remains unexplored [19]. From an evolutionary perspective, identifying genomic regions associated with specific phenotypic traits can help disentangle the effects of early domestication and historical selective breeding on camel health and welfare, based on the biological functions of the associated genes ('domestication syndrome' hypothesis) [20].

The present study performs genome-wide association studies to identify genomic regions that may regulate the expression of traits such as zoometrics, biomechanics, and behaviour in dromedary camels. The results will complement the list of genetic variants previously reported to be associated with morphometric traits in dromedaries [17] after screening a larger number of animals and a higher-density SNP array. They will also serve to explore the genomic basis of biomechanical and behavioural traits in this livestock species for the first time. Overall, the insights gained from this research will inform future breeding programs, guide conservation efforts, and enrich our understanding of the genomic features of early domestication and modern selection in camels.

Results and discussion

Altogether, the results from the present study are consistent with the well-documented concept of 'domestication syndrome' in mammals. This term refers to a set of morphological, physiological, and behavioral traits that result from genetic changes associated with domestication. Specifically for Old World camels, Fitak, Mohandesan [21] detected recent, positive selection for 107 candidate genes linked to neural crest deficiencies and altered thyroid hormone-based signaling in camel species. Such candidate genes underlie traits collectively recognized within the just-referred 'domestication syndrome'. Upon examination, we found that none of the candidate genes identified in our study have been reported as genes under positive selection in the dromedary camel populations in existing literature [22–24]. Hence, our study contributes novel insights into candidate genes that may be relevant for understanding the effects of domestication and modern selection in dromedaries. Furthermore, the fact that none of our candidate genes have been reported as under positive selection in previous studies highlights the genetic diversity among dromedary camels inhabiting at different locations and suggest that different populations may experience unique selective pressures or adaptations. In turn, we emphasize the importance of examining different camel populations to understand their specific evolutionary trajectories.

Genotypic clustering reflects intergroup differentiation and slight introgression

Principal Component Analysis (PCA) based on 50 K genotypes revealed that raising farm is a significant clustering criterion for study dromedary camels (Fig. 1; PC1 and PC2 explained 16.5% and 8.4% of genetic variation, respectively). For example, farms 2 and 3 are the largest reserves of Canarian dromedaries, and they are genetically connected through the exchange of living animals

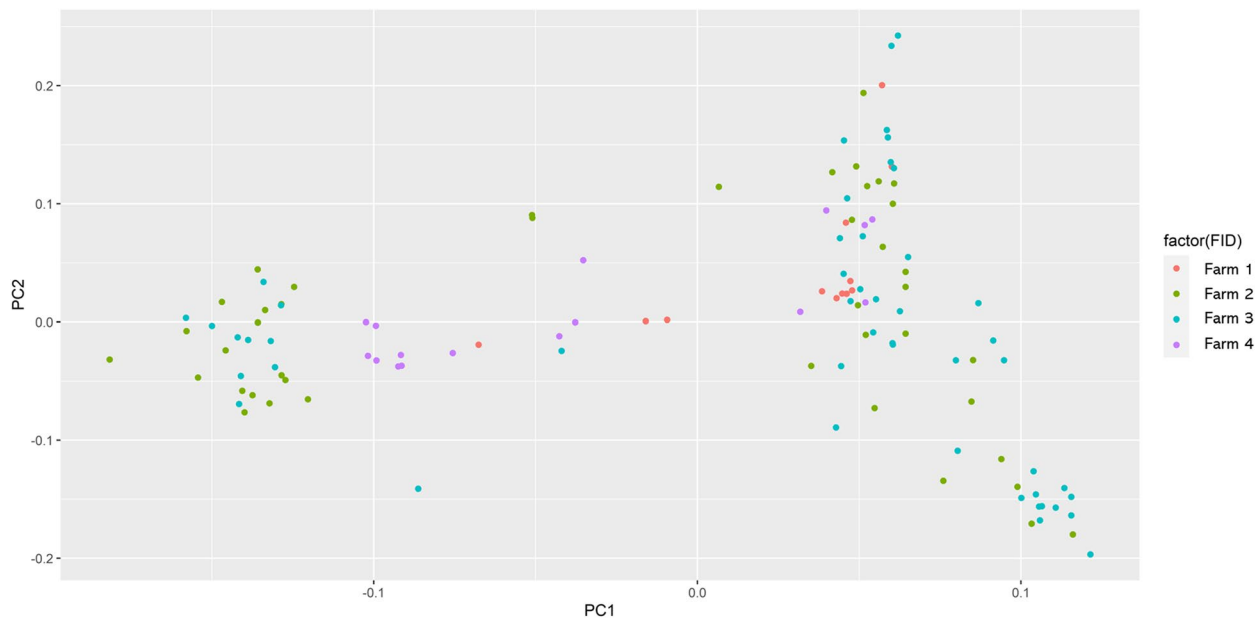


Fig. 1 Principal components analysis (PCA) results displaying the clustering of 120 Canarian dromedary camels raised at 4 farms according to their 50 K genotypes

for breeding purposes. At these farms, dromedaries are sorted into subgroups based on their sex, age, and phenotypic characters. Farm-specific breeding programs might have led to the selection of distinct genetic lines, thereby causing the observed genetic differentiation between animals within Farm 2 and 3. Additionally, environmental factors and selective pressures unique to each farm could also contribute to the genetic divergence observed within these subpopulations. These farms are the primary source for living animals of Farm 1 [25, 26] and the rest of Europe. In contrast, Farm 4's genetic connection with the others is less frequent, which may explain its relatively unique genetic structure. Such genetic differentiation among Canarian camel's breeding farms coincide with the results of previous researches aimed at studying phenotypic diversity for camel zoometrics on the same study population [27]. Instead, the factor 'farm' did not have a significant discriminatory effect on camel biomechanical and behavioral performance [28, 29]. Camel gait is a highly conserved ancestral trait [30]. Concerning behavior, this trait tends to be evolutionarily conserved across populations [31], especially when environmental conditions and management practices are relatively uniform across farms. Since behavioral traits are often influenced by essential genetic factors mostly linked to survival and adaptation, they can remain stable despite genetic differentiation.

This clustering pattern also serves to explain the phenotypic diversity encountered in the study sample. Descriptive statistics (minimum (Min), maximum (Max), mean, and standard deviation (SD)) for the 12 phenotypes

recorded in 120 dromedary camels are presented in Table 1. High variability, particularly for body morphometrics and Intelligence Quotient, was noted. Both environmental pressures and functional specialization at domestic scenarios significantly influence the morphology and psyche of the animals [32]. However, physical performance traits showed little variation, likely due to the conserved nature of camel trait [30].

Overall, the structure of the study animal population suggests that human-driven selection of dromedary camels maintains assortative mating for size and behavior akin to natural populations [33]. Under the condition of gregarious animal species, assortative mating is crucial for optimizing energy investment towards reproduction and survival in arid environments.

Linkage disequilibrium pattern supports the suitability of the study population and SNP array density for accurate high-resolution genomic mapping

The LD decay plot is shown in Fig. 2. Moderate LD ($r^2=0.20$) is present at 100 kb between markers. This finding aligns with the LD patterns described by Bahbahani [34], where similar distances for moderate LD ($r^2=0.25$) were observed. Differences in LD patterns may arise from variations in sample size, genomic coverage, and genotyping methods.

Assuming a size for camel genome of 2.2 Gb, achieving saturation of the genome with an average resolution

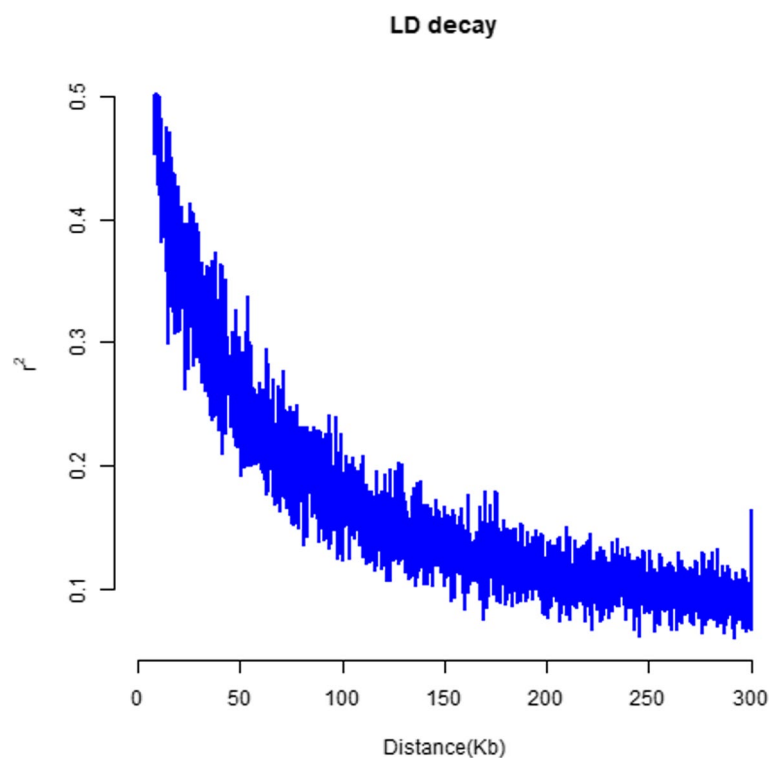
Table 1 Descriptive statistics (minimum (Min), maximum (Max), mean, and standard deviation (SD)) for the zoometrics, biomechanics and behaviour traits recorded in 120 dromedary camels

Phenotype category	Trait/unit of measurement	Min	Max	Mean \pm SD
Zoometrics	Length (cm)	48.22	80.98	70.46 \pm 5.03
	Height (cm)	54.93	77.03	64.66 \pm 3.96
	Width (cm)	26.79	41.78	36.01 \pm 2.72
	Perimeter/girth (cm)	52.06	83.77	72.02 \pm 5.18
Biomechanics	Acceleration (coefficients of the cubic regression model)	-0.06	0.05	0.00 \pm 0.02
	Velocity (coefficients of the cubic regression model)	-0.06	0.05	-0.01 \pm 0.02
	Displacement (coefficients of the cubic regression model)	-0.10	0.07	-0.04 \pm 0.05
	Spatial position (coefficients of the cubic regression model)	-0.31	-0.06	-0.22 \pm 0.07
Behaviour	Copying styles (intensity of response)	1	5	2.88 \pm 0.68
	General cognition (intensity of response)	1	5	3.99 \pm 0.52
	Intelligence (intensity of response)	1	5	4.00 \pm 0.58
	Intelligence Quotient (IQ) (points)	92.04	137.97	102.36 \pm 8.17

of 100 kb would necessitate 22,000 fully informative SNPs. It means that a minimum of 22,000 SNPs are required to cover the genome and capture LD information for genome-wide association studies in camels [35]. Our study exceeds this threshold, with 49,632 SNPs retained after quality control, and all 120 animals included in the analysis.

Variations in camel body morphometrics might correlate to increased prevalence and incidence of sensory and cognitive impairments

Seven SNPs at genome-wide level (Fig. 3) and twenty-nine SNPs at chromosome-wide level were significantly associated with zoometrics-related traits in dromedary camels. Twenty-three different candidate genes were identified (Table 2). None of these genes overlap with

**Fig. 2** Linkage disequilibrium (LD) decay plot depicted from pairwise LD values (r^2) against genetic distance (Kb) between genomic markers across dromedary camel genome

those reported previously in other studies that investigated the genetic basis of growth and morphometric traits in dromedaries [17, 18, 36]. Although future functional studies will allow for a more precise confirmation of gene functions in dromedaries, we rely on previous association studies in multiple species (mammals and zebrafish), considering that genome-wide association signals are enriched in orthologous genes associated in other species, as suggested by Gualdrón Duarte, Yuan [37].

PVRIG, *STAG3*, *GAL3ST4*, *TRAPPC14*, and *LAMTOR4* genes affect width and perimeter/girth measurements in dromedary camels. These genes are associated with various conditions in humans, mice and zebrafish. They are linked to neurodegenerative and neuropsychiatric processes, which can affect eye size and morphology, cause microcephaly, and lead to abnormal ciliogenesis, cilia instability, reduced thigmotactic behavior, decreased locomotor activity, and hyperactivity. They are also related to immune response, including lymphadenomegalia and T-cell function. Regarding reproductive performance, they are associated with infertility, abnormal embryo size, and embryonic/preweaning lethality. Additionally, these genes are connected to cell cycle regulation and skeletal structure, impacting bone density and rib morphology [38–43].

Four (*ZCCHC8*, *RSRC2*, *KNTC1*, and *U6*) and seven (*TENM2*, *LYN*, *RPS20*, *SNORD54*, *MOS*, *KCNV2*, and *PUM3*) additional genes regulate width and perimeter/girth measurements, respectively. *ZCCHC8*, *RSRC2*, *KNTC1*, and *U6* genes are linked to neoplastic processes, decreased reproductive performance, narrow eye opening, motor neuron diseases, retinitis pigmentosa, poikiloderma with neutropenia, and recessive intellectual

disability in humans and mice [38, 44–47]. Instead, those genes that are specifically associated with perimeter/girth measurements in our study, are widely recognized for their implication on morpho-functional alterations at sensory-neural tissues and organs, neoplastic processes, immune structures, and pigmentation in humans and animal models. Concretely, *TENM2*, *KCNV2*, and *PUM3* genes are associated with abnormalities at retina ganglion, cone-rod distribution, eye size, visual cortex, superior colliculus, and lateral geniculate nucleus in humans, mice, and zebrafish [48–50]. The just-referred structures play essential roles in normal visual processing and orienting motor responses, visuospatial attention, and perceptual decision-making. *LYN* gene is related to a wide range of neoplastic processes in humans [45] and immune dysfunctions in mice [51, 52]. In addition, abnormal pigmentations at the skin, epidermis, ear, and tail, as well as decreased exploratory behaviour, are phenotypes associated to genomic variability in *RPS20* gene in mice [53, 54]. Interestingly, the association of *RPS20* gene with perimeter/girth measurements in dromedary camels provides further evidence to support the correlations previously found between body morphometrics (height at withers, chest girth, and hump girth) and weight, leadership behaviour, and coat pigmentation in dromedary camels by Iglesias Pastrana, Navas González [25]. *MOS* gene, however, has been mostly associated to reduced reproductive performance and cell cycle alterations in mice [55, 56].

Lastly, phenotypic variability for length measurements was found to be controlled by other seven candidate genes (*PCDH15*, *NEASC*, *SAMD12*, *SPAG16*, *POU2F2*, *ZNF574*, and *GRIK5*). *PCDH15*, *NEASC*, *SAMD12*, *POU2F2*, and *GRIK5* genes are associated with decreased

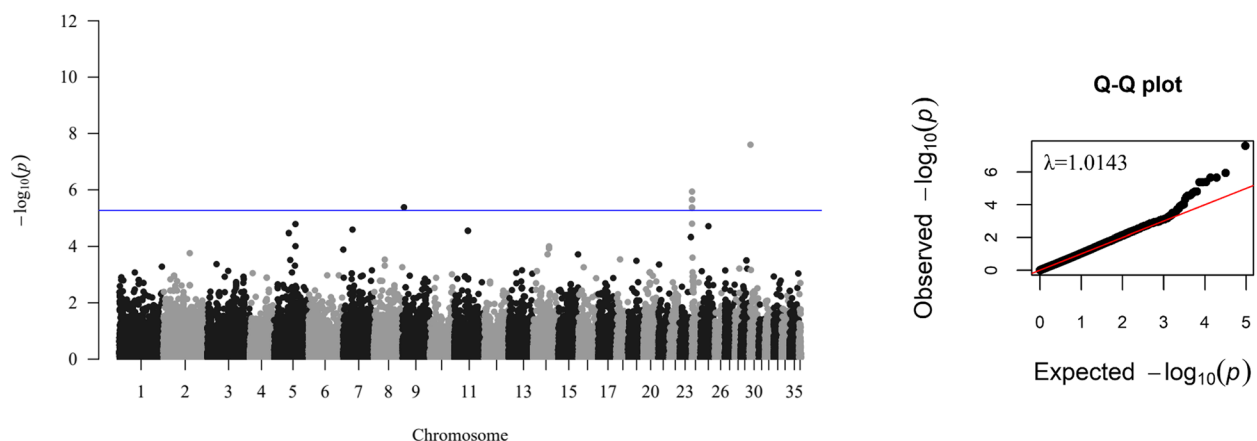


Fig. 3 Manhattan and Q-Q plots displaying the results of the genome-wide association study for zoometrics-related trait ‘Length’ in dromedary camels. Negative $\log_{10} P$ -values (y-axis) of the associations between SNPs and length phenotypes are plotted against the genomic location of each SNP marker (x-axis). Blue line represents the threshold of genome-wide significance after correction for multiple testing (q -value = 0.05)

Table 2 Genome- and chromosome-wide significant associations between SNP markers and zoometrics-related traits in dromedary camels

Level of significance	Trait	Chr ¹	Affy SNP ID ²	Pos ³	A1 ⁴	MAP ⁵	β ± SE ⁶	P-value	q-value ⁷	PVE ⁸	Candidate gene(s) name(s)
Genome-wide	Length	9	Affx-960,933,216	4,135,877	A	0.158	-3.573 ± 0.865	< 0.001	0.029	0.124	POU2F2, ZNF574, GRIK5
		24	Affx-960,963,086	1,257,593	A	0.125	-3.761 ± 0.818	< 0.001	0.029	0.150	
		24	Affx-960,997,693	1,337,164	A	0.138	-3.763 ± 0.772	< 0.001	0.026	0.165	
		24	Affx-960,963,092	1,382,174	A	0.217	-3.033 ± 0.634	< 0.001	0.029	0.160	
		24	Affx-960,963,093	1,401,421	A	0.138	-3.763 ± 0.772	< 0.001	0.026	0.165	
		24	Affx-960,963,095	1,421,441	A	0.225	-3.232 ± 0.624	< 0.001	0.026	0.182	
		30	Affx-960,969,899	2,519,875	A	0.025	-10.050 ± 1.784	< 0.001	0.001	0.209	
		5	Affx-960,920,909	41,408,799	A	0.496	2.375 ± 0.543	< 0.001	0.041	0.137	
		5	Affx-960,921,565	60,230,516	G	0.292	-2.664 ± 0.609	< 0.001	0.040	0.137	SPAG16
		9	Affx-960,933,216	4,135,877	A	0.158	-3.573 ± 0.865	< 0.001	0.008	0.124	POU2F2, ZNF574, GRIK5
Chromosome-wide	Length	11	Affx-960,940,074	38,938,407	A	0.017	-8.033 ± 2.057	< 0.001	0.030	0.112	PCDH15
		11	Affx-960,940,075	38,992,975	A	0.017	-8.033 ± 2.057	< 0.001	0.030	0.112	PCDH15
		23	Affx-960,962,923	32,418,534	A	0.358	-2.700 ± 0.594	< 0.001	0.043	0.146	NFASC
		24	Affx-960,963,086	1,257,593	A	0.125	-3.761 ± 0.818	< 0.001	4.7 × 10 ⁻⁰⁴	0.149	
		24	Affx-960,997,693	1,337,164	A	0.138	-3.763 ± 0.772	< 0.001	4.1 × 10 ⁻⁰⁴	0.165	
		24	Affx-960,997,694	1,345,978	G	0.259	-2.530 ± 0.590	< 0.001	1.4 × 10 ⁻⁰³	0.132	
		24	Affx-960,963,092	1,382,174	A	0.217	-3.033 ± 0.634	< 0.001	4.7 × 10 ⁻⁰⁴	0.160	
		24	Affx-960,963,093	1,401,421	A	0.138	-3.763 ± 0.772	< 0.001	4.1 × 10 ⁻⁰⁴	0.165	
		24	Affx-960,963,095	1,421,441	A	0.225	-3.232 ± 0.772	< 0.001	4.1 × 10 ⁻⁰⁴	0.182	
		24	Affx-960,963,155	2,769,311	A	0.421	-1.924 ± 0.531	< 0.001	0.020	0.098	
Perimeter/girth		25	Affx-960,964,966	23,461,775	A	0.042	-5.868 ± 1.217	< 0.001	0.020	0.162	SAMD12
		30	Affx-960,969,899	2,519,875	A	0.025	-10.050 ± 1.784	< 0.001	1.783 × 10 ⁻⁰⁵	0.209	
		3	Affx-960,916,079	90,597,288	A	0.038	7.662 ± 1.715	< 0.001	0.040	0.142	
		4	Affx-960,918,746	47,376,072	A	0.087	-4.751 ± 1.156	< 0.001	0.045	0.123	KCNV2
		4	Affx-960,988,889	47,393,983	G	0.209	-3.398 ± 0.791	< 0.001	0.045	0.133	KCNV2, PUM3
		18	Affx-960,956,138	25,972,784	A	0.442	-3.123 ± 0.650	< 0.001	0.008	0.161	PYRIG, STAG3, GAL3ST4, TRAPPC14, LAMTOR4
		22	Affx-960,960,917	9,913,664	G	0.158	-3.320 ± 0.747	< 0.001	0.008	0.141	TENM2
		22	Affx-960,997,300	9,922,210	A	0.158	-3.115 ± 0.774	< 0.001	0.034	0.118	TENM2
		22	Affx-960,960,918	9,943,037	G	0.158	-3.115 ± 0.774	< 0.001	0.034	0.118	TENM2

Table 2 (continued)

Level of significance	Trait	Chr ¹	Affy SNP ID ²	Pos ³	A1 ⁴	MAF ⁵	$\beta \pm SE^6$	P-value	q-value ⁷	PVE ⁸	Candidate gene(s) name(s)
		29	Affx-960,968,839	3,727,916	A	0.317	2.449 ± 0.600	< 0.001	0.047	0.122	LYN, RPS20, SNORD54, MOS
		29	Affx-960,968,861	4,248,472	A	0.067	-4.675 ± 1.243	< 0.001	0.047	0.105	
		29	Affx-960,968,863	4,325,706	G	0.138	-3.630 ± 0.858	< 0.001	0.047	0.130	
		35	Affx-960,974,423	1,644,974	A	0.321	-3.096 ± 0.731	< 0.001	0.013	0.130	
	Width	18	Affx-960,956,138	25,972,784	A	0.442	-1.671 ± 0.365	< 0.001	0.041	0.148	PVRIG, STAG3, GAL3ST4, TRAPPC14, LAMTOR4
		32	Affx-960,972,422	18,441,303	G	0.129	-2.557 ± 0.494	< 0.001	0.005	0.182	ZCCHC8, RSRG2, KNTC1, U6

¹Chr: chromosome; ²SNP ID: Affymetrix SNP ID number; ³Pos: position in base pairs; ⁴A1: minor allele; ⁵MAF: minor allele frequency; ⁶ $\beta \pm SE$: allelic substitution effect \pm standard error; ⁷q-value: P-values corrected for multiple testing using a false discovery rate approach; ⁸PVE: proportion of variance in phenotype explained by a given SNP

general behaviour activity, quality of musculoskeletal movement and balance (proprioception), visual and hearing capacity, and immune function, as well as increased prevalence of neurodevelopmental disorders with central and peripheral motor dysfunction (i.e., hemorrhagic brain, abnormal synaptic transmission and postsynaptic currents, syndromic intellectual disability, and increased startle reflex and thermal nociceptive threshold) in humans, mice, rats, and zebrafish [57–65]. A missense variant in *PCDH15* gene is also responsible for the unexpectedly low number of homozygous haplotype carriers for two different Holstein haplotypes that are related to insemination success and neonatal survival in cattle [66]. On the other hand, *SPAG16* gene is linked to decreased reproductive performance [67–69] and increased prevalence of ciliary dyskinesia (PCD), a X-linked disorder that mainly affects respiratory tissues [70], in humans, mice, and cattle. *ZNF574* gene is a hub gene of adipose tissue metabolism in cattle [71] and tumor regulation in humans [72–74].

Developmental dysplasia and heart abnormalities may underlie decreased locomotor performance in dromedary camels

Twenty-four SNPs at the chromosome-wide level of significance were significantly associated with biomechanical traits in dromedary camels (Table 3). Eleven candidate genes, which can play potential roles in camels based on their known functions in other mammalian species/animal models (orthologous genes) [37], were identified. *MIR187*, *FBXO8*, and *TTC28* genes affect displacement and spatial position measurements. Altered expression of these genes correlates with diverse malignancies and the regulation of inflammation, cell stemness, insulin secretion, and embryonic development in humans and mice [75–77]. Furthermore, the downregulation of *MIR187* gene is linked to intellectual disability and temporal lobe epilepsy in humans and animal models [78, 79]. *FBXO8* gene is also involved in motor neuron degeneration in humans [80]. Additionally, *TTC28* gene is associated with bone and heart abnormalities in mice [53], and increased feed conservation ratio in pig [81].

Acceleration-related traits in dromedaries are controlled by six different genes (*PRSS56*, *CHRND*, *CHRNG*, *EIF4E2*, *EFHD1*, and *GRID1*). Loss of *PRSS56* gene function leads to impaired visual acuity in humans and mice [82]. *CHRND* and *CHRNG* gene mutations cause congenital myasthenic and multiple pterygium syndrome/fetal akinesia in humans, mice, zebrafish, and dogs [83–87]. Various mutant mice models for *EIF4E2* gene served to unraveling the role of this gene in the regulation of synaptic plasticity and autism spectrum disorder-associated behaviors [88]. In addition, Sun, Huang [89] and

Sun, Yang [90] founded that this gene was also associated with the response to exercise in buffalo and protects the heart against hypoxia in zebrafish. Similarly, mutant mice and wildtype (AB line) zebrafish were used to unravel the functional role of *EFHD1* gene in axonal morphogenesis, cardiac mitoflash activation, protection of cardiomyocytes from ischemia, and brain general development and function [91–93]. *GRID1* gene variants are linked to schizophrenia, bipolar disorder, intellectual disability, and spastic paraplegia in humans [94, 95]. Mice lacking *GRID1* gene suffer from sensorineural hearing loss [96].

Lastly, *MYLK4* gene controls velocity traits in dromedary camels. *MYLK4* gene polymorphisms are related to skeletal muscle metabolism and hypertrophic cardiomyopathy in mice [97, 98]; growth and meat tenderness traits cattle [99, 100], goat [101] and pig [102]; energy metabolism in muscle in Chinese perch [103]; and milk production traits in water buffalo [104].

Embryonic neurogenesis and neurodegeneration could shape the behavioural patterns and processes of dromedary camels

Behavioural traits in dromedaries were associated with nine SNPs at genome-wide level (Fig. 4) and fifty-five SNPs at chromosome-wide level of significance (Table 4). Thirty-eight novel candidate genes were identified. The potential role of these genes in dromedaries is presumed, until species-specific functional studies do exist, basing on the related information existing for orthologous genes in other multiple species [37].

CACNA1E gene was found to be associated with both cognition and intelligence-linked traits. Polymorphisms in this gene are linked to impaired glucose metabolism, motor dysfunction, and heightened fear/depression/anxiety-like behaviours in mice and rats [105–107]. Eleven other genes (*MZT1*, *BORA*, *DIS3*, *PIBF1*, *KLF5*, *KLF12*, *GPC5*, *ABCC4*, *ERCC5*, *DST*, and *CACNA1E*) were associated with intelligence traits. *MZT1*, *BORA*, *DIS3*, *PIBF1*, and *KLF5* are linked to syndromic intellectual disability and autism spectrum disorder in humans [108]. A homozygous haplotype-related loss-of-function variant has been also identified in bovine *DIS3*, most likely causing embryonic lethality [109]; and mutations in humans *DIS3* engrosses the list of risk factors for multiple myeloma [110]. *PIBF1* additionally regulates embryonic development and litter size in mice and sheep [111], and is associated with an increased incidence of alterations in neural tube closure/morphology and Joubert syndrome (varying degrees of physical, mental, and visual impairments) in animal models such as mice and frog [53, 112]. *KLF5* and *KLF12* mutant and wild-type mice are biased for the prognosis of cardiovascular diseases given their differential inner capabilities of structural remodeling of

Table 3 Genome- and chromosome-wide significant associations between SNP markers and biomechanical traits in dromedary camels

Level of significance	Trait	Chr ¹	Affy SNP ID ²	Pos ³	A1 ⁴	MAF ⁵	β ± SE ⁶	P-value	q-value ⁷	PVE ⁸	Candidate gene(s) name(s)
Chromosome-wide	Acceleration	1	Affx-960,987,276	49,067,023	A	0.013	-0.038 ± 0.008	< 0.001	0.041	0.142	
		5	Affx-960,922,793	90,882,617	G	0.042	-0.020 ± 0.004	< 0.001	0.036	0.131	PRRS56, CHRD, CHRN, EIF4E2, EFHD1
	Displacement	5	Affx-960,922,794	90,898,605	A	0.042	-0.020 ± 0.004	< 0.001	0.036	0.131	CHRD, CHRN, EIF4E2, EFHD1
		11	Affx-960,940,770	63,080,477	A	0.39	-0.008 ± 0.002	< 0.001	0.022	0.134	GRID1
	Spatial position	11	Affx-960,940,771	63,089,184	A	0.383	-0.009 ± 0.002	< 0.001	0.022	0.143	GRID1
		27	Affx-960,998,234	8,630,370	A	0.108	-0.012 ± 0.003	< 0.001	0.028	0.116	
		15	Affx-960,951,241	44,613,389	A	0.067	0.047 ± 0.009	< 0.001	0.008	0.172	
		24	Affx-960,963,406	7,360,225	A	0.062	0.037 ± 0.008	< 0.001	0.021	0.131	MIR187
		31	Affx-960,971,530	13,185,060	A	0.154	0.028 ± 0.007	< 0.001	0.022	0.117	FBXO8
		31	Affx-960,971,531	13,196,723	G	0.154	0.028 ± 0.007	< 0.001	0.022	0.117	FBXO8
32		Affx-960,998,920	5,642,595	G	0.1	0.037 ± 0.008	< 0.001	0.042	0.138	TTC28	
32		Affx-960,998,923	5,686,300	G	0.1	0.036 ± 0.008	< 0.001	0.042	0.130	TTC28	
Velocity	Spatial position	5	Affx-960,920,099	14,592,645	G	0.033	0.102 ± 0.021	< 0.001	0.028	0.160	U6
		5	Affx-960,920,103	14,777,622	A	0.033	0.102 ± 0.021	< 0.001	0.028	0.160	
	15	Affx-960,951,241	44,613,389	A	0.067	0.069 ± 0.014	< 0.001	0.018	0.162		
	24	Affx-960,963,406	7,360,225	A	0.062	0.054 ± 0.013	< 0.001	0.035	0.124	MIR187	
	31	Affx-960,971,530	13,185,060	A	0.154	0.042 ± 0.010	< 0.001	0.024	0.115	FBXO8	
	31	Affx-960,971,531	13,196,723	G	0.154	0.042 ± 0.010	< 0.001	0.024	0.115	FBXO8	
	32	Affx-960,998,920	5,642,595	G	0.1	0.057 ± 0.012	< 0.001	0.035	0.147	TTC28	
	32	Affx-960,998,923	5,686,300	G	0.1	0.05 ± 0.012	< 0.001	0.035	0.133	TTC28	
Velocity	9	Affx-960,935,451	60,922,008	G	0.183	-0.015 ± 0.003	< 0.001	0.037	0.136		
	20	Affx-960,958,073	1,522,955	A	0.312	-0.013 ± 0.003	< 0.001	0.030	0.130	MYLK4	

¹ Chr: chromosome; ² SNP ID: Affymetrix SNP ID number; ³ Pos: position in base pairs; ⁴ A1: minor allele; ⁵ MAF, minor allele frequency; ⁶ β ± SE: allelic substitution effect ± standard error; ⁷ q-value: P-values corrected for multiple testing using a false discovery rate approach; ⁸ PVE: proportion of variance in phenotype explained by a given SNP

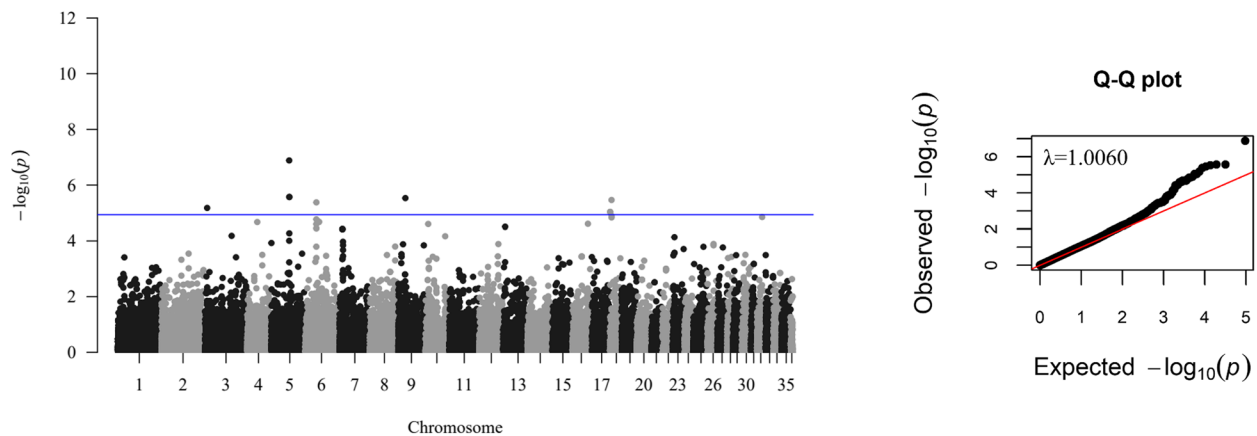


Fig. 4 Manhattan and Q-Q plots displaying the results of the genome-wide association study for behavioural trait 'Intelligence Quotient' in dromedary camels. Negative log₁₀ P-values (y-axis) of the associations between SNPs and IQ-related phenotypes are plotted against the genomic location of each SNP marker (x-axis). Blue line represents the threshold of genome-wide significance after correction for multiple testing (q -value=0.05)

the heart and blood vessels [113, 114], and the severity of clinical pancreatic cancer [115], respectively. *GPC5* and *ABCC4* genes mutations have been confirmed to be functionally implicated in skeletal and growth defects, neural tube closure defects, and predisposition to nephrotic syndrome in humans, pigs, frogs and zebrafish [116–119]. Further shreds of evidence ascertained that non-synonymous mutations in *ABCC4* gene ascribe to reproductive traits in cattle, buffalo, and pig [120], and resistance to paratuberculosis in cattle [121]. Heritable disorders resulting from mutations in the *ERCC5* gene include both cancer and neurodegenerative processes (intracranial malformations and cerebro-oculo-facio-skeletal syndrome) in humans and mice [122, 123]. *DST* gene has been also reported to be implicated in hereditary sensory and autonomic neuropathies in humans and mice [124].

Lastly, the Intelligence Quotient was regulated by twenty-seven genes. Such genes play significant roles in the self-renewal, early embryo development, and reprogramming of embryonic stem cells in mice [125], and predisposition to intellectual disability in rats (*TEX10*) [65]; prevalence and incidence of cardiovascular-renal-hepatic-pancreatic dysplasia in zebrafish, mice and humans (*INVS* and *PTPN18*) [53, 126, 127]; human and mice senescence and premature aging, which in turn can be implicated in the development of age-related neurodegenerative processes (*UBE2E3*) [128]; incidence of recessive ocular coloboma and neural tube defects in humans and mice (*SALL2*) [129, 130]; olfaction (*OR10G2*, *OR10G3*, *OR4E2*, and *OR4E1*) [131] and protection against caries (*TRAV4*) in humans [132]; increased risk of motor system dysfunctions

(i.e., amyotrophic lateral sclerosis and benign hereditary chorea) and several autoimmune diseases in *Drosophila*, humans and rats (*SCFD1*) [65, 133, 134]; high prevalence of progressive cochleo-vestibular dysfunction (reduced linear vestibular evoked potential and sensorineural hearing loss) in humans, mice and rats (*COCH*) [53, 65, 135]; thigmotaxis, hyperactivity, vertical activity, brain-lung-thyroid syndrome, severe intellectual disability, mild fever-sensitive seizure, developmental delay, spastic paraplegia, muscular atrophy, cardiovascular failure, microcephaly, and short stature, in humans and animal models (*STRN3*, *AP4S1*, *PUS7*, *ATP2A3*, *ZZEF1* and *PXN*) [53, 136–140]; regulation of neuronal differentiation and pathogenesis of Alzheimer disease in humans, mice and zebrafish (*ZNF536*, *UI* and *SRPK2*) [141–143]; muscle function, energy and redox metabolism during exercise in mice (*SIRT4*) [144]; incidence of diet-induced obesity and risk of diabetes and atherosclerosis in humans and mice (*PLA2G1B*) [145]; and incidence of abnormalities in neurocranium morphology, size and vascular perfusion in mice and rats (*MSII*) [53, 65].

Conclusions

The interindividual phenotypic variability in zoometrics, biomechanics and behaviour-related traits in dromedary camels is controlled by polygenic determinants that are located on multiple chromosomes. A total of 124 SNPs, mapped to 70 different candidate genes involved in synthesizing biological products, have been identified as significantly associated with these functional traits. These genes primarily regulate various neurodevelopmental processes and sensory perception. Our findings enhance

Table 4 Genome- and chromosome-wide significant associations between SNP markers and behavioural traits in dromedary camels

Level of significance	Trait	Chr ¹	Affy SNP ID ²	Pos ³	A1 ⁴	MAF ⁵	β ± SE ⁶	P-value	q-value ⁷	PVE ⁸	Candidate gene(s) name(s)
Genome-wide	Intelligence Quotient (IQ)	3	Affx-960,912,845	6,407,091	A	0.121	5.127 ± 1.086	< 0.001	0.045	0.156	
		5	Affx-960,921,228	51,633,138	A	0.013	17.266 ± 3.077	< 0.001	0.006	0.207	
		5	Affx-960,921,252	52,106,921	A	0.029	10.963 ± 2.178	< 0.001	0.033	0.174	
		5	Affx-960,991,234	52,118,548	A	0.029	10.963 ± 2.178	< 0.001	0.033	0.174	
		6	Affx-960,924,214	31,702,577	G	0.108	5.687 ± 1.126	0.002	0.033	0.175	TRAV3, TRAV4
		9	Affx-960,933,889	20,323,326	A	0.067	7.204 ± 1.421	< 0.001	0.033	0.176	ZNF536
Chromosome-wide	General cognition	18	Affx-960,955,268	956,822	A	0.188	4.542 ± 0.947	0.001	0.050	0.160	
		18	Affx-960,955,431	4,973,535	A	0.029	10.985 ± 2.216	0.001	0.033	0.170	
		21	Affx-960,960,559	24,771,582	A	0.321	0.300 ± 0.074	< 0.001	0.025	0.119	
		21	Affx-960,997,111	27,637,855	G	0.125	0.428 ± 0.108	< 0.001	0.026	0.114	CACNA1E
		21	Affx-960,960,611	27,655,130	G	0.132	0.448 ± 0.109	< 0.001	0.025	0.122	CACNA1E
		29	Affx-960,969,388	16,938,208	A	0.017	-1.087 ± 0.271	< 0.001	0.028	0.118	
		29	Affx-960,969,389	16,947,732	G	0.017	-1.087 ± 0.271	< 0.001	0.028	0.118	
		14	Affx-960,947,638	24,522,730	G	0.225	0.352 ± 0.078	< 0.001	0.013	0.145	
		14	Affx-960,947,639	24,548,084	G	0.225	0.352 ± 0.078	< 0.001	0.013	0.145	
		14	Affx-960,947,643	24,602,982	A	0.174	0.351 ± 0.090	0.001	0.050	0.110	
Intelligence		14	Affx-960,948,278	40,665,048	G	0.237	0.300 ± 0.080	< 0.001	0.013	0.106	MZT1, BORA, DIS3, PIBF1
		14	Affx-960,948,279	40,683,674	G	0.239	0.300 ± 0.080	< 0.001	0.013	0.107	BORA, DIS3, PIBF1
		14	Affx-960,948,284	40,782,683	G	0.287	0.281 ± 0.071	< 0.001	0.013	0.115	PIBF1
		14	Affx-960,994,388	40,827,573	A	0.225	0.295 ± 0.080	< 0.001	0.013	0.100	PIBF1, KLF5
		14	Affx-960,948,288	40,865,525	A	0.233	0.277 ± 0.077	< 0.001	0.013	0.097	PIBF1, KLF5
		14	Affx-960,948,289	40,904,517	A	0.221	0.276 ± 0.084	0.002	0.026	0.082	KLF5
		14	Affx-960,948,315	41,370,829	A	0.483	-0.275 ± 0.066	< 0.001	0.013	0.126	KLF12
		14	Affx-960,948,774	53,034,349	A	0.033	0.760 ± 0.201	< 0.001	0.022	0.106	
		14	Affx-960,948,863	54,869,550	G	0.055	0.571 ± 0.150	< 0.001	0.038	0.108	GPC5
		14	Affx-960,948,879	55,173,735	A	0.329	-0.300 ± 0.064	< 0.001	0.013	0.152	GPC5
		14	Affx-960,948,882	55,211,008	G	0.2	-0.333 ± 0.082	< 0.001	0.014	0.120	GPC5
		14	Affx-960,948,885	55,258,723	A	0.042	0.600 ± 0.176	0.001	0.050	0.087	GPC5
		14	Affx-960,948,980	57,425,357	A	0.171	0.304 ± 0.085	< 0.001	0.050	0.095	ABCC4
		14	Affx-960,949,196	62,777,326	A	0.217	0.280 ± 0.078	< 0.001	0.050	0.095	ERCC5
20	Affx-960,959,619	40,202,723	A	0.161	-0.392 ± 0.083	< 0.001	0.012	0.157	DST		

Table 4 (continued)

Level of significance	Trait	Chr ¹	Affy SNP ID ²	Pos ³	A1 ⁴	MAF ⁵	β ± SE ⁶	P-value	q-value ⁷	PVE ⁸	Candidate gene(s) name(s)
		21	Affx-960,960,559	24,771,582	A	0.321	0.272 ± 0.071	< 0.001	0.045	0.107	
		21	Affx-960,997,111	27,637,855	G	0.125	0.458 ± 0.010	< 0.001	0.013	0.152	CACNA1E
		21	Affx-960,960,611	27,655,130	G	0.132	0.468 ± 0.010	< 0.001	0.013	0.156	CACNA1E
	Intelligence Quotient (IQ)	3	Affx-960,912,845	6,407,091	A	0.121	5.127 ± 1.086	< 0.001	0.020	0.156	
		4	Affx-960,918,124	28,991,717	A	0.037	9.061 ± 1.943	0.003	0.033	0.153	TEX10, INVS
		5	Affx-960,919,456	1,049,490	A	0.437	3.094 ± 0.850	< 0.001	0.048	0.010	PTPN18
		5	Affx-960,921,228	51,633,138	A	0.013	17.266 ± 3.077	< 0.001	0.001	0.207	
		5	Affx-960,921,239	51,800,375	G	0.079	5.625 ± 1.467	< 0.001	0.048	0.109	
		5	Affx-960,921,248	52,001,303	G	0.037	8.440 ± 1.956	< 0.001	0.032	0.134	UBE2E3
		5	Affx-960,921,252	52,106,921	A	0.029	10.963 ± 2.178	< 0.001	0.002	0.174	
		5	Affx-960,991,234	52,118,548	A	0.029	10.963 ± 2.178	< 0.001	0.002	0.174	
		6	Affx-960,989,928	31,617,037	A	0.185	3.870 ± 0.976	< 0.001	0.049	0.115	SALL2, OR10G3, OR10G2, OR4E2, OR4E1
		6	Affx-960,989,929	31,635,047	G	0.216	3.832 ± 0.844	< 0.001	0.010	0.146	OR10G3, OR10G2, OR4E2, OR4E1, TRAV3, TRAV4
		6	Affx-960,924,213	31,691,628	G	0.259	3.883 ± 0.856	0.0015	0.010	0.146	OR4E1, TRAV3, TRAV4
		6	Affx-960,924,214	31,702,577	G	0.108	5.687 ± 1.126	0.0025	0.010	0.175	TRAV3, TRAV4
		6	Affx-960,924,215	31,712,105	A	0.267	3.731 ± 0.846	0.0017	0.012	0.140	TRAV3, TRAV4
		6	Affx-960,924,499	38,911,834	G	0.05	7.893 ± 1.728	0.0013	0.010	0.148	SCFD1
		6	Affx-960,989,972	38,963,797	A	0.05	7.893 ± 1.728	0.0013	0.010	0.148	COCH, STRN3
		6	Affx-960,924,503	39,058,843	G	0.05	7.893 ± 1.728	0.0013	0.010	0.148	STRN3, U6, AP4S1
		7	Affx-960,926,977	8,701,842	A	0.271	4.424 ± 1.072	< 0.001	0.028	0.124	PUS7, U1, SRPK2
		7	Affx-960,926,979	8,739,948	G	0.271	4.424 ± 1.072	< 0.001	0.028	0.124	PUS7, U1, SRPK2
		7	Affx-960,926,980	8,752,290	A	0.271	4.424 ± 1.072	< 0.001	0.028	0.124	PUS7, U1, SRPK2
		9	Affx-960,933,889	20,323,326	A	0.067	7.204 ± 1.421	< 0.001	0.005	0.176	ZNF536
		10	Affx-960,936,199	8,752,356	A	0.017	12.506 ± 2.788	< 0.001	0.042	0.143	
		16	Affx-960,952,985	44,513,833	A	0.017	12.547 ± 2.842	< 0.001	0.027	0.140	ATP2A3, ZZZEF1
		18	Affx-960,955,268	956,822	A	0.188	4.542 ± 0.947	0.0016	0.002	0.160	
		18	Affx-960,955,431	4,973,535	A	0.029	10.985 ± 2.216	< 0.001	0.002	0.170	
		18	Affx-960,955,432	4,981,762	G	0.034	8.685 ± 1.9	< 0.001	0.002	0.150	
		18	Affx-960,995,885	5,033,615	A	0.033	8.728 ± 1.9	< 0.001	0.002	0.150	
		32	Affx-960,999,045	15,037,248	A	0.013	16.120 ± 3.353	0.0014	0.007	0.161	PXN, U4, SIRT4, PLA2G1B, MS11

¹ Chr: chromosome; ²SNP ID: Affymetrix SNP ID number; ³Pos: position in base pairs; ⁴A1: minor allele; ⁵MAF: minor allele frequency; ⁶β ± SE: allelic substitution effect ± standard error; ⁷q-value: P-values corrected for multiple testing using a false discovery rate approach; ⁸PVE: proportion of variance in phenotype explained by a given SNP

the empirical understanding of the genomic features of early domestication and modern selection in dromedary camels, and will inform future sustainable breeding and conservation programs for this species. In particular, the integration of gene function analysis, genomics-based selection and proper sub-grouping of individuals based on phenotypic similarities (assortative natural behaviour) in human-controlled environments will greatly support efforts to preserve the health and welfare of camels.

Methods

Phenotype assessment and blood sampling

Between October 2019 and July 2020, one hundred twenty Canarian dromedary camels (70 males and 50 females; reared at 4 different semi-extensive farms (2 farms in Canary Islands and 2 farms in mainland Spain)) were phenotyped for body morphometrics, biomechanics, and behaviour related traits. A total of thirty zoometric measurements were taken from each animal as indicated by Iglesias Pastrana, Navas González [146]. Zoometric measurements included linear and tridimensional zoometric traits from head, neck, thorax and dorsum, hump, rump and tail, extremities, and feet. Such measurements were aggregated depending on their geometric nature into four phenotypic categories (length, height, width, and perimeter/girth measurements).

Regarding biomechanical performance traits, curve estimation regression statistics was applied to the individual motion measurements for eleven key kinematic variables at ten different anatomic regions, obtained through video analyses, to calculate the coefficients of the mathematical function that best described locomotor behaviour in dromedary camels (cubic function), as described in Pastrana, González [147]. The anatomic regions evaluated for their biomechanics were the cranial angle of the scapula, midway between acromion and head of the humerus (shoulder joint), olecranon (elbow joint), carpus and fetlock (metacarpophalangeal joint) on the forelimb, the iliac crest, greater trochanter of the femur (hip), stifle (knee) joint, point of the hock (tarsus), and fetlock (metatarsophalangeal joint) on the hindlimb. Kinematic variables recorded include acceleration, horizontal acceleration, horizontal position, horizontal velocity, total distance, total horizontal displacement, total vertical displacement, velocity, vertical acceleration, vertical position, and vertical velocity. Biomechanical performance traits were then sub-grouped in four different phenotypic categories, namely: acceleration, velocity, displacement, and spatial position measurements.

Behavioural traits included four phenotypic categories (copying styles, general cognition, intelligence, and Intelligence Quotient (IQ)). First, 'copying styles' category

comprised behavioural-type coping strategies (proactivity and reactivity displayed by leisure dromedaries in response to social stressors at man-made environments) [28]. Second, 'general cognition' category included traits such as dependence, trainability, cooperation, emotional stability, perseverance, get in/out of stables, and ease at handling. Strongly related, the phenotypic category of 'intelligence' is composed by the traits: concentration, curiosity, memory, stubbornness, docility, and alertness constituted. Copying styles, general cognition, and intelligence were evaluated through the application of an operant-conditioning problem-solving test. The last category, namely 'Intelligence Quotient' (IQ), is a psychometric construct calculated from the individual performance for the general cognition and intelligence related traits [148].

Immediately after individual phenotyping, a blood sample from each dromedary camel was collected through jugular venipuncture in 2 mL vials containing ethylenediaminetetraacetic acid (EDTA) and stored at -20 °C until genomic DNA extraction tasks. DNA was extracted using the QIAamp® DNA Mini Kit according to the manufacturer's protocol.

Genotyping and standard SNP genotype quality control

High-throughput, high density SNP genotyping array was used to generate the sequence data was used to generate the sequence data (Axiom Camelids Genotyping Array (Affymetrix, CA, USA)) as per the manufacturer's instructions. This chip contains 62,707 SNPs evenly distributed across the dromedary camel genome. The data related to SNP annotation are included in Supplementary Table S 1. Standard quality control procedures were applied to the SNP genotypes using PLINK v1.9. Markers with a call rate below 0.90, a minor allele frequency (MAF) less than 0.02, a Hardy-Weinberg equilibrium p value less than 0.001, and those mapping to sex chromosomes were excluded from the analysis. Additionally, individuals with a genotype call rate lower than 0.95 were susceptible to being excluded from further analyses. After implementing these quality control measures, a total of 49,632 SNPs and all the animals initially included were retained for subsequent analyses. A principal component analysis (PCA) was run with PLINK v1.9 to explore the genetic population structure.

Linkage disequilibrium

Linkage disequilibrium (LD), the degree of non-random association of alleles between loci or correlation between genotypes of markers, was estimated for each pairwise combination of SNPs using the software PopLDdecay [149]. According to McKay, Schnabel [35], in QTL mapping, r^2 is favored as the measure of linkage

disequilibrium because it quantifies the degree of information that one locus (which may be a quantitative trait or disease-related and potentially unobservable) can provide about another locus. Consequently, r^2 is useful for estimating the number of loci required in association studies.

Genome-wide association study (GWAS) for zoometrics, biomechanics, and behaviour-related traits

Following the methodology of Macri, Luigi-Sierra [150], genotype-phenotype association analysis was conducted using the Genome-wide Efficient Mixed-Model Association (GEMMA) v0.98.1 package [151]. The phenotypic information used was the mean quantitative value per each categorical phenotype described and animal (length, height, width, perimeter/girth, acceleration, velocity, displacement, spatial position, copying styles, general cognition, intelligence, and Intelligence Quotient). For each phenotype, a univariate linear mixed model was fitted according to the following formula:

$$y = W\alpha + x\beta + u + \varepsilon; u \sim \text{MVN}_n(0, \lambda \tau^{-1} K),$$

$$\text{and } \varepsilon \sim \text{MVN}_n(0, \tau^{-1} I_n)$$

where y represents an n -vector of zoometrics-, biomechanics- and behaviour-related phenotypes for $n = 120$ individuals; W is an $n \times c$ matrix ($c =$ number of fixed factors) that includes a column of 1s and the fixed effects, namely, sex (2 levels) and age category (3 levels); α is a c -vector denoting the corresponding fixed effects, including the intercept; x represents a n -vector of marker genotypes; β represents the marker's effect size (allele substitution effect); u is a n -vector of random individual effects that are normally distributed, $u \sim N(0, \lambda \tau^{-1} K)$, where τ^{-1} denotes the residual error variance, λ represents the ratio between the two variance components, and K is a SNP genotypes-derived $n \times n$ known relatedness matrix. Lastly, ε represents a n -vector of errors, and I_n represents an $n \times n$ identity matrix; while MVN_n depicts the multivariate normal distribution with n dimensions. P -values obtained for each association were adjusted for multiple testing with the False Discovery Rate (FDR) method (q -value). In the context of genome-wide association studies (GWAS), the q -value represents the false discovery rate for a given p -value. It estimates the proportion of false positives among the results with a p -value less than or equal to the q -value. In other words, the q -value helps to control for multiple comparisons and reduces the likelihood of reporting false positives, providing a more accurate measure of statistical significance in large-scale studies. Associations with a p -value and

q -value below 0.05 were deemed statistically significant. Manhattan plots were generated using the "qqman" R package. The estimation of the proportion of phenotypic variance that can be explained by a specific SNP (PVE) was performed using the following formula [152]:

$$\text{PVE} = \frac{2\beta^2 \text{MAF} (1 - \text{MAF})}{2\beta^2 \text{MAF} (1 - \text{MAF}) + [\text{se}(\beta)]^2 2N \text{MAF} (1 - \text{MAF})}$$

where β represents the SNP variant estimated effect size, $\text{se}(\beta)$ represents the β estimate standard error, MAF denotes the minor allele SNP frequency, and N is the size of the sample. The P lambda function from the R package QCEWA was used to calculate lambda (λ) inflation factors, and quantile-quantile (Q-Q) plots were generated using the ggqqplot function. The Biomart tool from Ensembl was used to retrieve genes located within a flanking region of ± 50 kb of the significant SNPs [17].

Supplementary Information

The online version contains supplementary material available at <https://doi.org/10.1186/s12917-024-04263-w>.

Supplementary Material 1.

Acknowledgements

The authors would also like to thank 'Aires Africanos' Eco-tourism Company, Oasis Park Fuerteventura, and 'Camelus' Camellos de Almería, for their direct technical help and assistance.

Authors' contributions

C.I.P, F.J.N.G., E.C. and J.V.D.B. conceived the project and designed the study. C.I.P, F.J.N.G. and J.V.D.B. carried out the phenotypic data collection. M.M., A.M.M. and E.C. completed the DNA extractions. C.I.P, F.J.N.G., M.M. and A.M.M. conducted the statistical analyses. C.I.P. and F.J.N.G. wrote the manuscript. All authors contributed to the editing and refinement of the final manuscript.

Funding

The present research was carried out in the financing framework of the international project CA.RA.VA.N - "Toward a Camel Transnational Value Chain" (Reference APCIN-2016-00011-00-00) and during the covering period of a pre-doctoral contract (FPU Fellowship) funded by the Spanish Ministry of Science and Innovation and a Ramón y Cajal Post-Doctoral Contract with the reference MCIN/AEI/<https://doi.org/10.13039/501100011033> and the European Union "NextGenerationEU"/PRTR.

Availability of data and materials

Phenotypes and genotypes of dromedary camels involved in this study are available from the Figshare <https://figshare.com/account/login#/projects/212105>.

Declarations

Ethics approval and consent to participate

All methods are reported in accordance with ARRIVE guidelines. Experimental protocols were exempt from approval as credited by The Spanish Ministry of Economy and Competitiveness through the Royal Decree Law 53/2013 and its credited entity, the Ethics Committee of Animal Experimentation from the University of Córdoba, permitted the application of the protocols present in this study as cited in the 5th section of its 2nd article, as the animals assessed were used for credited zootechnical use. This national Decree follows the

European Union Directive 2010/63/UE, from the 22 September of 2010. All farms included in the study followed specific codes of good practices and therefore, the animals received humane care in compliance with the national guide for the care and use of laboratory and farm animals in research. All owners gave their informed consent for the inclusion of their animals before they participated in the study. The study was conducted in accordance with the Declaration of Helsinki.

Consent for publication

Not applicable.

Competing interests

The authors declare no competing interests.

Received: 24 June 2024 Accepted: 3 September 2024

Published online: 18 September 2024

References

- Abri MAA, Faye B. Genetic improvement in dromedary camels: challenges and opportunities. *Front Genet.* 2019;10:167.
- Burger PA, Ciani E, Faye B. Old World camels in a modern world—a balancing act between conservation and genetic improvement. *Anim Genet.* 2019;50(6):598–612.
- Faye B. Role, distribution and perspective of camel breeding in the third millennium economies. *Emir J Food Agric.* 2015;27(4):318–27.
- Pastrana CI, González FJN, Ciani E, Ariza AG, Bermejo JVD. A tool for functional selection of leisure camels: Behaviour breeding criteria may ensure long-term sustainability of a European unique breed. *Res Vet Sci.* 2021;140:142–52.
- Rúa A, Caballero A. *Genética cuantitativa*. Madrid: Editorial Síntesis; 2017.
- Bitaraf Sani M, Zare Harofte J, Banabazi MH, Esmailkhanian S, Shafei Naderi A, Salim N, et al. Genomic prediction for growth using a low-density SNP panel in dromedary camels. *Sci Rep.* 2021;11(1):1–14.
- Alhaddad H, Alhajeri BH. Cdrom archive: a gateway to study camel phenotypes. *Front Genet.* 2019;10: 48.
- König S, Simianer H, Willam A. Economic evaluation of genomic breeding programs. *J Dairy Sci.* 2009;92(1):382–91.
- Rothschild MF. Porcine genomics delivers new tools and results: this little piggy did more than just go to market. *Genet Res.* 2004;83(1):1–6.
- Hayes BJ, Bowman PJ, Chamberlain AJ, Goddard ME. Invited review: genomic selection in dairy cattle: Progress and challenges. *J Dairy Sci.* 2009;92(2):433–43.
- Almathen F, Elbir H, Bahbahani H, Mwacharo J, Hanotte O. Polymorphisms in MC1R and ASIP genes are associated with coat color variation in the arabian camel. *J Hered.* 2018;109(6):700–6.
- Nowier AM, El-Metwaly HA, Ramadan SI. Genetic variability of tyrosinase gene in Egyptian camel breeds and its association with udder and body measurements traits in Maghrebi camel breed. *Gene Rep.* 2020;18:100569.
- Ishag I, Reissmann M, Eltaher H, Ahmed M. Polymorphisms of tyrosinase gene (exon 1) and its impact on coat color and phenotypic measurements of Sudanese Camel breeds. *Sci J Anim Sci.* 2013;2(5):109–15.
- Abdel-Aziem SH, Abdel-Kader HA, Alam SS, Othman OE. Detection of MspI polymorphism and the single nucleotide polymorphism (SNP) of GH gene in camel breeds reared in Egypt. *Afr J Biotechnol.* 2015;14(9):752–7.
- Al-Sharif M, Radwan H, Hendam B, Ateya A. DNA polymorphisms of FGFBP1, leptin, κ -casein, and α s1-casein genes and their association with reproductive performance in dromedary she-camels. *Theriogenology.* 2022;178:18–29.
- Bitaraf Sani M, Zare Harofte J, Banabazi MH, Faraz A, Esmailkhanian S, Naderi AS, et al. Identification of candidate genes for pigmentation in camels using genotyping-by-sequencing. *Animals.* 2022;12(9):1095.
- Bitaraf Sani M, Karimi O, Burger PA, Javanmard A, Roudbari Z, Mohajer M, et al. A genome-wide association study of morphometric traits in dromedaries. *Vet Med Sci.* 2023;9:1781–90.
- Sabahat S, Nadeem A, Brauning R, Thomson PC, Khatkar MS. Genome wide association study for growth in Pakistani dromedary camels using genotyping-by-sequencing. *Anim Biosci.* 2022;36(7):1010–21.
- Iglesias Pastrana C. Genetic and functional characterization of the 'Canarian Camel' breed. Doctoral dissertation. Cordoba: University of Cordoba; 2023.
- Wilkins AS, Wrangham RW, Fitch WT. The domestication syndrome in mammals: a unified explanation based on neural crest cell behavior and genetics. *Genetics.* 2014;197(3):795–808.
- Fitak RR, Mohandesan E, Corander J, Yadamsuren A, Chuluunbat B, Abdelhadi O, et al. Genomic signatures of domestication in Old World camels. *Commun Biology.* 2020;3(1):316.
- Bahbahani H, Alfoudari A, Al-Ateeqi A, Al Abri M, Almathen F. Positive selection footprints and haplotype distribution in the genome of dromedary camels. *Animal.* 2024;18(3):101098.
- Al Abri M, Alfoudari A, Mohammad Z, Almathen F, Al-Marzooqi W, Al-Hajri S, et al. Assessing genetic diversity and defining signatures of positive selection on the genome of dromedary camels from the southeast of the Arabian Peninsula. *Front Veterinary Sci.* 2023;10:1296610.
- Bahbahani H, Musa HH, Wragg D, Shuipei ES, Almathen F, Hanotte O. Genome diversity and signatures of selection for production and performance traits in dromedary camels. *Front Genet.* 2019;10:893.
- Iglesias Pastrana C, Navas González FJ, Ciani E, Arando Arbulu A, Delgado Bermejo JV. The Youngest, the Heaviest and/or the Darkest? Selection potentialities and determinants of Leadership in Canarian Dromedary camels. *Animals.* 2021;11(10):2886.
- Iglesias Pastrana C, Navas González FJ, Ciani E, Nogales Baena S, Delgado Bermejo JV. Camel Genetic Resources Conservation through Tourism: a key Sociocultural Approach of Camelback Leisure Riding. *Animals.* 2020;10(9):1703.
- Iglesias Pastrana C, Navas González FJ, Ciani E, González Ariza A, Nogales Baena S, Delgado Bermejo JV. Evidence of subpopulation diversification and traces of introgression within canarian camel breed zoometric standard: scope and opportunities for selection. *Italian J Anim Sci.* 2024;23(1):467–79.
- Pastrana CI, González FJN, Ciani E, McLean AK, Bermejo JVD. Behavioural-type coping strategies in leisure dromedary camels: factors determining reactive vs. proactive responses. *Appl Anim Behav Sci.* 2024;272:106186.
- Iglesias Pastrana C, Navas González FJ, Ciani E, Marín Navas C, Delgado Bermejo JV. Determination of breeding criteria for gait proficiency in leisure riding and racing dromedary camels: a stepwise multivariate analysis of factors predicting overall biomechanical performance. *Front Veterinary Sci.* 2024;10:1297430.
- Webb S. Locomotor evolution in camels. *Forma et functio An International Journal of Functional Biology.* 1972;5:99–112.
- Dalos J, Royauté R, Hedrick AV, Dochtermann NA. Phylogenetic conservation of behavioural variation and behavioural syndromes. *J Evol Biol.* 2022;35(2):311–21.
- Hansen Wheat C, Fitzpatrick JL, Rogell B, Temrin H. Behavioural correlations of the domestication syndrome are decoupled in modern dog breeds. *Nat Commun.* 2019;10(1):2422.
- Janicke T, Marie-Orleach L, Aubier TG, Perrier C, Morrow EH. Assortative mating in animals and its role for speciation. *Am Nat.* 2019;194(6):865–75.
- Bahbahani H. Long-range linkage disequilibrium events on the genome of dromedary camels as a signal of epistatic and directional positive selection. *Heliyon.* 2024;10(14):e34343.
- McKay SD, Schnabel RD, Murdoch BM, Matukumalli LK, Aerts J, Coppie W, et al. Whole genome linkage disequilibrium maps in cattle. *BMC Genet.* 2007;8:1–12.
- Bitaraf Sani M, Zare Harofte J, Banabazi MH, Esmailkhanian S, Shafei Naderi A, Salim N, et al. Genomic prediction for growth using a low-density SNP panel in dromedary camels. *Sci Rep.* 2021;11(1):7675.
- Gualdrón Duarte JL, Yuan C, Gori A-S, Moreira GC, Takeda H, Coppieters W, et al. Sequenced-based GWAS for linear classification traits in Belgian

- blue beef cattle reveals new coding variants in genes regulating body size in mammals. *Genet Selection Evol.* 2023;55(1):83.
38. Informatics MG, the International Mouse Phenotyping Consortium (IMPC). Obtaining and loading phenotype annotations from the International Mouse Phenotyping Consortium (IMPC) database. IMPC database release. 2014.
 39. Llano E, Gomez HL, García-Tuñón I, Sánchez-Martín M, Caburet S, Barbero JL, et al. STAG3 is a strong candidate gene for male infertility. *Hum Mol Genet.* 2014;23(13):3421–31.
 40. Ward A, Hopkins J, McKay M, Murray S, Jordan PW. Genetic interactions between the meiosis-specific cohesin components, STAG3, REC8, and RAD21L. *G3: Genes, Genomes, Genetics.* 2016;6(6):1713–24.
 41. Tirozzi A, Quiccione MS, Cerletti C, Donati MB, de Gaetano G, Iacoviello L, et al. A Multi-trait Association Analysis of Brain Disorders and platelet traits identifies Novel susceptibility loci for Major Depression, Alzheimer's and Parkinson's Disease. *Cells.* 2023;12(2):245.
 42. Murter B, Pan X, Ophir E, Alteber Z, Azulay M, Sen R, et al. Mouse PVRIG has CD8+T cell-specific coinhibitory functions and dampens antitumor immunity. *Cancer Immunol Res.* 2019;7(2):244–56.
 43. Zaqout S, Kaindl AM. Autosomal recessive primary microcephaly: not just a small brain. *Front Cell Dev Biology.* 2022;9:3635.
 44. Gable DL, Gaysinskaya V, Atik CC, Talbot CC, Kang B, Stanley SE, et al. ZCCHC8, the nuclear exosome targeting component, is mutated in familial pulmonary fibrosis and is required for telomerase RNA maturation. *Genes Dev.* 2019;33(19–20):1381–96.
 45. Sondka Z, Bamford S, Cole CG, Ward SA, Dunham I, Forbes SA. The COSMIC Cancer Gene Census: describing genetic dysfunction across all human cancers. *Nat Rev Cancer.* 2018;18(11):696–705.
 46. Wu Y, Liu W, Chen J, Liu S, Wang M, Yang L, et al. Nuclear exosome targeting complex core factor Zcchc8 regulates the degradation of LINE1 RNA in early embryos and embryonic stem cells. *Cell Rep.* 2019;29(8):2461–72 e6.
 47. Mroczek S, Dziembowski A. U6 RNA biogenesis and disease association. *Wiley Interdisciplinary Reviews: RNA.* 2013;4(5):581–92.
 48. Young TR, Bourke M, Zhou X, Oohashi T, Sawatari A, Fässler R, et al. Tenm2 is required for the generation of binocular visual circuits. *J Neurosci.* 2013;33(30):12490–509.
 49. Wissinger B, Schaich S, Baumann B, Bonin M, Jägle H, Friedburg C, et al. Large deletions of the KCN2V gene are common in patients with cone dystrophy with supernormal rod response. *Hum Mutat.* 2011;32(12):1398–406.
 50. Thisse B, Pflumio S, Fürthauer M, Loppin B, Heyer V, Degraeve A, et al. Expression of the zebrafish genome during embryogenesis. ZFIN direct data submission. 2001;11:1979–87.
 51. Lamagna C, Scapini P, van Ziffle JA, DeFranco AL, Lowell CA. Hyperactivated MyD88 signaling in dendritic cells, through specific deletion of Lyn kinase, causes severe autoimmunity and inflammation. *Proceed National Acad Sciences.* 2013;110(35):E3311–20.
 52. Verhagen AM, Wallace ME, Goradia A, Jones SA, Croom HA, Metcalf D, et al. A kinase-dead allele of Lyn attenuates autoimmune disease normally associated with Lyn deficiency. *J Immunol.* 2009;182(4):2020–9.
 53. Informatics MG. Obtaining and loading phenotype annotations from the International Mouse Phenotyping Consortium (IMPC) database. IMPC database release. 2014. <https://www.mousephenotype.org/>.
 54. McGowan KA, Li JZ, Park CY, Beaudry V, Tabor HK, Sabnis AJ, et al. Ribosomal mutations cause p53-mediated dark skin and pleiotropic effects. *Nat Genet.* 2008;40(8):963–70.
 55. Choi T, Fukasawa K, Zhou R, Tessarollo L, Borror K, Resau J, et al. The Mos/mitogen-activated protein kinase (MAPK) pathway regulates the size and degradation of the first polar body in maturing mouse oocytes. *Proc Natl Acad Sci.* 1996;93(14):7032–5.
 56. Colledge W, Carlton M, Udy G, Evans M. Disruption of c-mos causes parthenogenetic development of unfertilized mouse eggs. *Nature.* 1994;370(6484):65–8.
 57. Alagramam KN, Murcia CL, Kwon HY, Pawlowski KS, Wright CG, Woychik RP. The mouse Ames Waltzer hearing-loss mutant is caused by mutation of Pcdh15, a novel protocadherin gene. *Nat Genet.* 2001;27(1):99–102.
 58. Goodman L, Zallocchi M. Integrin $\alpha 8$ and Pcdh15 act as a complex to regulate cilia biogenesis in sensory cells. *J Cell Sci.* 2017;130(21):3698–712.
 59. Ahmed ZM, Riazuddin S, Aye S, Ali RA, Venselaar H, Anwar S, et al. Gene structure and mutant alleles of PCDH15: nonsyndromic deafness DFNB23 and type 1 Usher syndrome. *Hum Genet.* 2008;124:215–23.
 60. Pillai AM, Thaxton C, Pribisko AL, Cheng JG, Dupree JL, Bhat MA. Spatiotemporal ablation of myelinating glia-specific neurofascin (NfascNF155) in mice reveals gradual loss of paranodal axoglial junctions and concomitant disorganization of axonal domains. *J Neurosci Res.* 2009;87(8):1773–93.
 61. Cen Z, Jiang Z, Chen Y, Zheng X, Xie F, Yang X, et al. Intronic pentanucleotide TTTCA repeat insertion in the SAMD12 gene causes familial cortical myoclonic tremor with epilepsy type 1. *Brain.* 2018;141(8):2280–8.
 62. Corcoran LM, Koentgen F, Dietrich W, Veale M, Humbert PO. All known in vivo functions of the Oct-2 transcription factor require the C-terminal protein domain. *J Immunol.* 2004;172(5):2962–9.
 63. Koromina M, Flitton M, Blockley A, Mellor IR, Knight HM. Damaging coding variants within kainate receptor channel genes are enriched in individuals with schizophrenia, autism and intellectual disabilities. *Sci Rep.* 2019;9(1):19215.
 64. Unlu G, Gamazon ER, Qi X, Levic DS, Bastarache L, Denny JC, et al. GRIK5 genetically regulated expression associated with eye and vascular phenomes: discovery through iteration among biobanks, electronic health records, and zebrafish. *Am J Hum Genet.* 2019;104(3):503–19.
 65. Twigger S, Lu J, Shimoyama M, Chen D, Pasko D, Long H, et al. Rat genome database (RGD): mapping disease onto the genome. *Nucleic Acids Res.* 2002;30(1):125–8.
 66. Häfliger IM, Spengeler M, Seefried FR, Drögemüller C. Four novel candidate causal variants for deficient homozygous haplotypes in holstein cattle. *Sci Rep.* 2022;12(1):5435.
 67. Sun T, Pei S, Liu Y, Hanif Q, Xu H, Chen N, et al. Whole genome sequencing of simmental cattle for SNP and CNV discovery. *BMC Genomics.* 2023;24(1):179.
 68. Zhang Z, Zariwala MA, Mahadevan MM, Caballero-Campo P, Shen X, Escudier E, et al. A heterozygous mutation disrupting the SPAG16 gene results in biochemical instability of central apparatus components of the human sperm axoneme. *Biol Reprod.* 2007;77(5):864–71.
 69. Escalier D. Knockout mouse models of sperm flagellum anomalies. *Hum Reprod Update.* 2006;12(4):449–61.
 70. Andjelkovic M, Minic P, Vreca M, Stojiljkovic M, Skakic A, Sovtic A, et al. Genomic profiling supports the diagnosis of primary ciliary dyskinesia and reveals novel candidate genes and genetic variants. *PLoS ONE.* 2018;13(10):e0205422.
 71. Wang X, Wang J, Raza SHA, Deng J, Ma J, Qu X, et al. Identification of the hub genes related to adipose tissue metabolism of bovine. *Front Veterinary Sci.* 2022;9:9.
 72. De Wilde B, Beckers A, Lindner S, Kristina A, De Preter K, Depuydt P, et al. The mutational landscape of MYCN, Lin28b and ALKF1174L driven murine neuroblastoma mimics human disease. *Oncotarget.* 2018;9(9):8334.
 73. Zhang J, Wu X, Huang L. ZNF574 promotes ovarian Cancer Cell Proliferation and Migration through regulating AKT and AMPK Signaling pathways. *Annals Clin Lab Sci.* 2022;52(4):611–20.
 74. Berg M, Ågesen TH, This-Evensen E, Merok MA, Teixeira MR, Vatn MH, et al. Distinct high resolution genome profiles of early onset and late onset colorectal cancer integrated with gene expression data identify candidate susceptibility loci. *Mol Cancer.* 2010;9(1):1–14.
 75. Lin S-C, Kao S-Y, Chang J-C, Liu Y-C, Yu E-H, Tseng S-H, et al. Up-regulation of miR-187 modulates the advances of oral carcinoma by targeting BARX2 tumor suppressor. *Oncotarget.* 2016;7(38):61355.
 76. Lasorsa VA, Montella A, Cantalupo S, Tirelli M, de Torres C, Aveic S, et al. Somatic mutations enriched in cis-regulatory elements affect genes involved in embryonic development and immune system response in neuroblastoma. *Cancer Res.* 2022;82(7):1193–207.
 77. Tonne JM, Sakuma T, Deeds MC, Munoz-Gomez M, Barry MA, Kudva YC, et al. Global gene expression profiling of pancreatic islets in mice during streptozotocin-induced β -cell damage and pancreatic Glp-1 gene therapy. *Dis Models Mech.* 2013;6(5):1236–45.
 78. Ünalp A, Coskunpinar E, Gunduz K, Pekuz S, Baysal BT, Edizer S, et al. Detection of deregulated miRNAs in childhood epileptic encephalopathies. *J Mol Neurosci.* 2022;72(6):1234–42.

79. Cattani AA, Allene C, Seifert V, Rosenow F, Henshall DC, Freiman TM. Involvement of micro RNA s in epileptogenesis. *Epilepsia*. 2016;57(7):1015–26.
80. Cronin S, Berger S, Ding J, Schymick JC, Washecka N, Hernandez DG, et al. A genome-wide association study of sporadic ALS in a homogenous Irish population. *Hum Mol Genet*. 2008;17(5):768–74.
81. Borowska A, Reyher H, Wimmers K, Varley PF, Szwaczkowski T. Detection of pig genome regions determining production traits using an information theory approach. *Livest Sci*. 2017;205:31–5.
82. Paylakhi S, Labelle-Dumais C, Tolman NG, Sellarole MA, Seymens Y, Saunders J, et al. Müller glia-derived PRSS56 is required to sustain ocular axial growth and prevent refractive error. *PLoS Genet*. 2018;14(3):e1007244.
83. Vogt J, Harrison BJ, Spearman H, Cossins J, Vermeer S, ten Cate LN, et al. Mutation analysis of CHRNA1, CHRN1, CHRND, and RAPSN genes in multiple pterygium syndrome/fetal akinesia patients. *Am J Hum Genet*. 2008;82(1):222–7.
84. Bonanno C, Rodolico C, Töpf A, Foti FM, Liu W-W, Beeson D, et al. Severe congenital myasthenic syndrome associated with novel biallelic mutation of the CHRND gene. *Neuromuscul Disord*. 2020;30(4):336–9.
85. Etard C, Behra M, Ertzer R, Fischer N, Jesuthasan S, Blader P, et al. Mutation in the δ -subunit of the nAChR suppresses the muscle defects caused by lack of Dystrophin. *Dev Dynamics*. 2005;234(4):1016–25.
86. Blakey TJ, Michaels JR, Guo LT, Hodshon AJ, Shelton GD. Congenital myasthenic syndrome in a mixed breed dog. *Front Veterinary Sci*. 2017;4:173.
87. Vogt J, Morgan NV, Rehal P, Favre L, Brueton LA, Becker K, et al. CHRNG genotype–phenotype correlations in the multiple pterygium syndromes. *J Med Genet*. 2012;49(1):21–6.
88. Wiebe S, Meng XQ, Kim SH, Zhang X, Lacaille JC, Aguilar-Valles A, et al. The eIF4E homolog 4EHP (eIF4E2) regulates hippocampal long-term depression and impacts social behavior. *Mol Autism*. 2020;11:1–16.
89. Sun T, Huang G-y, Wang Z-h, Teng S-h, Cao Y-h, Sun J-l, et al. Selection signatures of Fuzhong Buffalo based on whole-genome sequences. *BMC Genomics*. 2020;21:1–10.
90. Sun L, Yang H, He D, Chen J, Dong Z, Luo S, Zhang M. Mammalian eIF4E2-GSK3 β maintains basal phosphorylation of p53 to resist senescence under hypoxia. *Cell Death Disease*. 2022;13(5):459.
91. Ulisse V, Dey S, Rothbard DE, Zeevi E, Gokhman I, Dadosh T, et al. Regulation of axonal mitogenesis by the mitochondrial protein Efhf1. *Life Sci Alliance*. 2020;3(7):e202000753.
92. Eberhardt DR, Lee SH, Yin X, Balynas AM, Rekatte EC, Kraiss JN, et al. EFHD1 ablation inhibits cardiac mitoflash activation and protects cardiomyocytes from ischemia. *J Mol Cell Cardiol*. 2022;167:1–14.
93. Wasilewska I, Gupta RK, Palchevska O, Kuźnicki J. Identification of zebrafish calcium toolkit genes and their expression in the brain. *Genes*. 2019;10(3):230.
94. Benamer N, Marti F, Lujan R, Hepp R, Aubier TG, Dupin A, et al. GluD1, linked to schizophrenia, controls the burst firing of dopamine neurons. *Mol Psychiatry*. 2018;23(3):691–700.
95. Ung DC, Pietrancosta N, Badillo EB, Raux B, Tapken D, Zlatanovic A, et al. GRID1/GluD1 homozygous variants linked to intellectual disability and spastic paraplegia impair mGlu1/5 receptor signaling and excitatory synapses. *Mol Psychiatry*. 2024;29:1205–15.
96. De Luca P, Scarpa A, Ralli M, Tassone D, Cassandro C, Simone M, et al. Immune-mediated Association between Celiac Disease and Sensorineural hearing loss: a systematic narrative review. *Turkish J Gastroenterol*. 2022;33(4):273.
97. Huang W, Kazmierczak K, Zhou Z, Aguilar-Pulido V, Narasimhan G, Szczesna-Cordary D. Gene expression patterns in transgenic mouse models of hypertrophic cardiomyopathy caused by mutations in myosin regulatory light chain. *Arch Biochem Biophys*. 2016;601:121–32.
98. Sakakibara I, Yanagihara Y, Himori K, Yamada T, Sakai H, Sawada Y, et al. Myofiber androgen receptor increases muscle strength mediated by a skeletal muscle splicing variant of Mylk4. *Iscience*. 2021;24(4):102303.
99. Aytekin İ, Bayraktar M, Sakar ÇM, Ünal İ. Association between MYLK4 gene polymorphism and growth traits at different age stages in Anatolian black cattle. *Animal Biotechnol*. 2020;31(6):555–60.
100. Won K, Kim D, Hwang I, Lee H-K, Oh J-D. Genome-wide association studies on collagen contents trait for meat quality in Hanwoo. *J Anim Sci Technol*. 2023;65(2):311.
101. Shi S-Y, Li L-J, Zhang Z-J, Wang E-Y, Wang J, Xu J-W, et al. Copy number variation of MYLK4 gene and its growth traits of *Capra hircus* (goat). *Animal Biotechnol*. 2020;31(6):532–7.
102. Fontanesi L, Schiavo G, Galimberti G, Calò D, Russo V. A genomewide association study for average daily gain in Italian large White pigs. *J Anim Sci*. 2014;92(4):1385–94.
103. Wu P, Chen L, Cheng J, Pan Y, Zhu X, Bao L, et al. The miRNA expression profile directly reflects the energy metabolic differences between slow and fast muscle with nutritional regulation of the Chinese perch (*Siniperca chuatsi*). *Comp Biochem Physiol A Mol Integr Physiol*. 2021;259:111003.
104. Du C, Deng T, Zhou Y, Ye T, Zhou Z, Zhang S, et al. Systematic analyses for candidate genes of milk production traits in water buffalo (*Bubalus Bubalis*). *Anim Genet*. 2019;50(3):207–16.
105. Smith MA, Katsouri L, Virtue S, Choudhury AI, Vidal-Puig A, Ashford ML, et al. Calcium channel CaV2.3 subunits regulate hepatic glucose production by modulating leptin-induced excitation of arcuate pro-opiomelanocortin neurons. *Cell Rep*. 2018;25(2):278–87. e4.
106. Rijkers K, Mescheriakova J, Majoie M, Lemmens E, van Wijk X, Philippen M, et al. Polymorphisms in CACNA1E and Camk2d are associated with seizure susceptibility of Sprague–Dawley rats. *Epilepsy Res*. 2010;91(1):28–34.
107. Huang C, Yang X, Zeng B, Zeng L, Gong X, Zhou C, et al. Proteomic analysis of olfactory bulb suggests CACNA1E as a promoter of CREB signaling in microbiota-induced depression. *J Proteom*. 2019;194:132–47.
108. Cosemans N, Vandenhove L, Maljaars J, Van Esch H, Devriendt K, Baldwin A, et al. ZNF462 and KLF12 are disrupted by a de novo translocation in a patient with syndromic intellectual disability and autism spectrum disorder. *Eur J Med Genet*. 2018;61(7):376–83.
109. Häfliger IM, Seefried FR, Drögemüller C. Reverse genetic screen for deleterious recessive variants in the local simmental cattle Population of Switzerland. *Animals*. 2021;11(12):3535.
110. Boyle EM, Ashby C, Tytarenko RG, Deshpande S, Wang H, Wang Y, et al. BRAF and DIS3 mutations associate with adverse outcome in a long-term follow-up of patients with multiple myeloma. *Clin Cancer Res*. 2020;26(10):2422–32.
111. Tao L, He X, Wang F, Pan L, Wang X, Gan S, et al. Identification of genes associated with litter size combining genomic approaches in Luzhong mutton sheep. *Anim Genet*. 2021;52(4):545–9.
112. Ott T, Kaufmann L, Granzow M, Hinderhofer K, Bartram CR, Theiß S, et al. The frog *Xenopus* as a model to study Joubert syndrome: the case of a human patient with compound heterozygous variants in PIBF1. *Front Physiol*. 2019;10:134.
113. Shindo T, Manabe I, Fukushima Y, Tobe K, Aizawa K, Miyamoto S, et al. Krüppel-like zinc-finger transcription factor KLF5/BTEB2 is a target for angiotensin II signaling and an essential regulator of cardiovascular remodeling. *Nat Med*. 2002;8(8):856–63.
114. Takeda N, Manabe I, Uchino Y, Eguchi K, Matsumoto S, Nishimura S, et al. Cardiac fibroblasts are essential for the adaptive response of the murine heart to pressure overload. *J Clin Investig*. 2010;120(1):254–65.
115. He Z, Guo X, Tian S, Zhu C, Chen S, Yu C, et al. MicroRNA-137 reduces stemness features of pancreatic cancer cells by targeting KLF12. *J Experimental Clin Cancer Res*. 2019;38:1–16.
116. de Pontual L, Yao E, Callier P, Favre L, Drouin V, Cariou S, et al. Germline deletion of the miR-17~92 cluster causes skeletal and growth defects in humans. *Nat Genet*. 2011;43(10):1026–30.
117. Okamoto K, Tokunaga K, Doi K, Fujita T, Suzuki H, Katoh T, et al. Common variation in GPC5 is associated with acquired nephrotic syndrome. *Nat Genet*. 2011;43(5):459–63.
118. Bassuk AG, Muthuswamy LB, Boland R, Smith TL, Hulstrand AM, Northrup H, et al. Copy number variation analysis implicates the cell polarity gene glypican 5 as a human spina bifida candidate gene. *Hum Mol Genet*. 2013;22(6):1097–111.
119. Ma C, Khederzadeh S, Adeola AC, Han X-M, Xie H-B, Zhang Y-P. Whole genome resequencing reveals an association of ABCC4 variants with preaxial polydactyly in pigs. *BMC Genomics*. 2020;21:1–13.
120. Li J, Liu J, Liu S, Plastow G, Zhang C, Wang Z, et al. Integrating RNA-seq and GWAS reveals novel genetic mutations for buffalo reproductive traits. *Anim Reprod Sci*. 2018;197:290–5.
121. Sanchez M-P, Guatteo R, Davergne A, Saout J, Grohs C, Deloche M-C, et al. Identification of the ABCC4, IER3, and CBFA2T2 candidate genes

- for resistance to paratuberculosis from sequence-based GWAS in Holstein and Normande dairy cattle. *Genet Selection Evol.* 2020;52(1):1–17.
122. Zhu M-L, Wang M, Cao Z-G, He J, Shi T-Y, Xia K-Q, et al. Association between the ERCC5 Asp1104His polymorphism and cancer risk: a meta-analysis. *PLoS ONE.* 2012;7(7):e36293.
 123. Kvarnung M, Taylan F, Nilsson D, Anderlid BM, Malmgren H, Lagerstedt-Robinson K, et al. Genomic screening in rare disorders: New mutations and phenotypes, highlighting ALG14 as a novel cause of severe intellectual disability. *Clin Genet.* 2018;94(6):528–37.
 124. Ferrier A, Sato T, De Repentigny Y, Gibeault S, Bhanot K, O'Meara RW, et al. Transgenic expression of neuronal dystonin isoform 2 partially rescues the disease phenotype of the dystonia musculorum mouse model of hereditary sensory autonomic neuropathy VI. *Hum Mol Genet.* 2014;23(10):2694–710.
 125. Ding J, Huang X, Shao N, Zhou H, Lee D-F, Faiola F, et al. Tex10 coordinates epigenetic control of super-enhancer activity in pluripotency and reprogramming. *Cell Stem Cell.* 2015;16(6):653–68.
 126. Otto EA, Schermer B, Obara T, O'Toole JF, Hiller KS, Mueller AM, et al. Mutations in INVS encoding inversin cause nephronophthisis type 2, linking renal cystic disease to the function of primary cilia and left-right axis determination. *Nat Genet.* 2003;34(4):413–20.
 127. Simons M, Gloy J, Ganner A, Bullerkotte A, Bashkurov M, Krönig C, et al. Inversin, the gene product mutated in nephronophthisis type II, functions as a molecular switch between wnt signaling pathways. *Nat Genet.* 2005;37(5):537–43.
 128. Plafker KS, Zyla K, Berry W, Plafker SM. Loss of the ubiquitin conjugating enzyme UBE2E3 induces cellular senescence. *Redox Biol.* 2018;17:411–22.
 129. Kelberman D, Islam L, Lakowski J, Bacchelli C, Chanudet E, Lescai F, et al. Mutation of SALL2 causes recessive ocular coloboma in humans and mice. *Hum Mol Genet.* 2014;23(10):2511–26.
 130. Böhm J, Buck A, Borozdin W, Mannan AU, Matysiak-Scholze U, Adham I, et al. Sall1, sall2, and sall4 are required for neural tube closure in mice. *Am J Pathol.* 2008;173(5):1455–63.
 131. Lif Holgerson P, Hasslöf P, Esberg A, Haworth S, Domellöf M, West CE, et al. Genetic Preference for Sweet Taste in Mothers Associates with Mother-Child Preference and Intake. *Nutrients.* 2023;15(11):2565.
 132. Briseño-Ruiz J, Shimizu T, Deeley K, Dizak PM, Ruff TD, Faraco IM, et al. Role of TRAV locus in low caries experience. *Hum Genet.* 2013;132:1015–25.
 133. Borg R, Purkiss A, Cacciottolo R, Herrera P, Cauchi RJ. Loss of amyotrophic lateral sclerosis risk factor SCFD1 causes motor dysfunction in *Drosophila*. *Neurobiol Aging.* 2023;126:67–76.
 134. Li CY, Yang TM, Ou RW, Wei QQ, Shang HF. Genome-wide genetic links between amyotrophic lateral sclerosis and autoimmune diseases. *BMC Med.* 2021;19:1–11.
 135. Usami S-i, Takahashi K, Yuge I, Ohtsuka A, Namba A, Abe S, et al. Mutations in the COCH gene are a frequent cause of autosomal dominant progressive cochleo-vestibular dysfunction, but not of Meniere's disease. *Eur J Hum Genet.* 2003;11(10):744–8.
 136. Lenaerts L, Reynhout S, Verbinen I, Laumonnier F, Toutain A, Bonnet-Brilhault F, et al. The broad phenotypic spectrum of PPP2R1A-related neurodevelopmental disorders correlates with the degree of biochemical dysfunction. *Genet Sci.* 2021;23(2):352–62.
 137. Hardies K, May P, Djémié T, Tarta-Arsene O, Deconinck T, Craiu D, et al. Recessive loss-of-function mutations in AP4S1 cause mild fever-sensitive seizures, developmental delay and spastic paraplegia through loss of AP-4 complex assembly. *Hum Mol Genet.* 2015;24(8):2218–27.
 138. De Brouwer AP, Abou Jamra R, Körstel N, Soyris C, Polla DL, Safra M, et al. Variants in PUS7 cause intellectual disability with speech delay, microcephaly, short stature, and aggressive behavior. *Am J Hum Genet.* 2018;103(6):1045–52.
 139. Hossain MB, Islam MK, Adhikary A, Rahaman A, Islam MZ. Bioinformatics Approach to identify significant biomarkers, drug targets Shared between Parkinson's Disease and bipolar disorder: a pilot study. *Bioinform Biol Insights.* 2022;16:1177932221079232.
 140. Ruzicka L, Howe DG, Ramachandran S, Toro S, Van Slyke CE, Bradford YM, et al. The Zebrafish Information Network: new support for non-coding genes, richer gene ontology annotations and the Alliance of Genome resources. *Nucleic Acids Res.* 2019;47(D1):D867–73.
 141. Bai B. U1 snRNP alteration and neuronal cell cycle reentry in Alzheimer disease. *Front Aging Neurosci.* 2018;10:75.
 142. Hong Y, Chan CB, Kwon I-S, Li X, Song M, Lee H-P, et al. SRPK2 phosphorylates tau and mediates the cognitive defects in Alzheimer's disease. *J Neurosci.* 2012;32(48):17262–72.
 143. Qin Z, Ren F, Xu X, Ren Y, Li H, Wang Y, et al. ZNF536, a novel zinc finger protein specifically expressed in the brain, negatively regulates neuron differentiation by repressing retinoic acid-induced gene transcription. *Mol Cell Biol.* 2009;29(13):3633–43.
 144. Han Y, Zhou S, Coetzee S, Chen A. SIRT4 and its roles in energy and redox metabolism in health, disease and during exercise. *Front Physiol.* 2019;10:1006.
 145. Hollie NI, Konanah ES, Goodin C, Hui DY. Group 1B phospholipase A2 inactivation suppresses atherosclerosis and metabolic diseases in LDL receptor-deficient mice. *Atherosclerosis.* 2014;234(2):377–80.
 146. Iglesias Pastrana C, Navas González FJ, Ciani E, Camacho Vallejo ME, Delgado Bermejo JV. Bayesian Linear regression and natural logarithmic correction for Digital Image-based extraction of Linear and Tridimensional Zoometrics in Dromedary camels. *Mathematics.* 2022;10(19):3453.
 147. Iglesias Pastrana C, Navas González FJ, Osman T, Ciani E, Delgado Bermejo JV. Curve estimation regression analysis to identify the model that best fits camel biomechanics applications for selective breeding. In: Proceedings of the 6th Conference of the International Society of Camelid Research and Development (ISOCARD) - 2023: The Role of Camel in Food Security and Economic Development. Al Ahsa: King Faisal University; 2023. p. 161.
 148. González FJN, Vidal JJ, Jurado JML, McLean AK, Bermejo JVD. Dumb or smart asses? Donkey's (*Equus asinus*) cognitive capabilities share the heritability and variation patterns of human's (*Homo sapiens*) cognitive capabilities. *J Veterinary Behav.* 2019;33:63–74.
 149. Zhang C, Dong S-S, Xu J-Y, He W-M, Yang T-L. PopLDdecay: a fast and effective tool for linkage disequilibrium decay analysis based on variant call format files. *Bioinformatics.* 2019;35(10):1786–8.
 150. Macri M, Luigi-Sierra MG, Guan D, Delgado JV, Alvarez JF, Amills M et al. Univariate and multivariate genome-wide association studies for hematological traits in Murciano-Granadina goats. *Anim Genet.* 2023;54:491–9.
 151. Zhou X, Stephens M. Efficient multivariate linear mixed model algorithms for genome-wide association studies. *Nat Methods.* 2014;11(4):407–9.
 152. Shim H, Chasman DI, Smith JD, Mora S, Ridker PM, Nickerson DA, et al. A multivariate genome-wide association analysis of 10 LDL subfractions, and their response to statin treatment, in 1868 caucasians. *PLoS ONE.* 2015;10(4):e0120758.

Publisher's note

Springer Nature remains neutral with regard to jurisdictional claims in published maps and institutional affiliations.